Food Chemistry: X 18 (2023) 100706

Contents lists available at ScienceDirect

Food Chemistry: X

journal homepage: www.sciencedirect.com/journal/food-chemistry-x

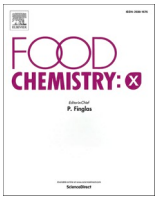

Purification and identification of oligosaccharides from *Cimicifuga heracleifolia* Kom. rhizomes

Liangnan Cui [a], Jing Wu [a], Xiang Wang [a], Xiaotong Yang [a], Zixin Ye [a], Kevin H. Mayo [b], Lin Sun [a], Yifa Zhou [a,*]

[a] *Engineering Research Center of Glycoconjugates, Ministry of Education, Jilin Provincial Key Laboratory on Chemistry and Biology of Changbai Mountain Natural Drugs, School of Life Sciences, Northeast Normal University, Changchun 130024, China*

[b] *Department of Biochemistry, Molecular Biology and Biophysics, University of Minnesota, 6-155 Jackson Hall, Minneapolis, MN 55455, USA*

ARTICLE INFO

Keywords:
Cimicifuga heracleifolia Kom.
Fructo-oligosaccharides
Purification
Structural elucidation

ABSTRACT

Even though *Cimicifuga* sp. is widely used in functional foods around the world, the content and structure of its oligosaccharides remain unclear. Here, we isolated a mixture of oligosaccharides from *Cimicifuga heracleifolia* Kom. rhizomes with a yield of 9.5% w/w. Twenty-six oligosaccharide monomers from the mixture were purified using optimized SEC and HILIC techniques. The oligosaccharides were identified as belonging to two groups by using HPAEC-PAD, MALDI-TOF-MS, NMR and GC–MS methylation analyses. One group belongs to sucrose and inulin type fructo-oligosaccharides (FOS) {β-D-Fru*f*-(2 → 1)-[β-D-Fru*f*-(2 ↔ 1)]$_{n=1\text{-}12}$-α-D-Glc*p*} with a 3–14 degree of polymerization (DP). Oligosaccharides in the other group belong to the inulo-*n*-ose type FOS {β-D-Fru*f*-(2 → 1)-[β-D-Fru*f*-(2 → 1)]$_{m=0\text{-}12}$-β-D-Fru*p*} with a DP of 2–14. This appears to be the first time that these oligosaccharides have been purified from *Cimicifuga heracleifolia* Kom., thus providing useful information concerning the utilization of *Cimicifuga heracleifolia* Kom. in functional foods.

Introduction

Cimicifuga heracleifolia Kom. that belongs to the genus *Cimicifuga* in the family Ranunculaceae, is commonly known in Chinese as "Sheng Ma". "Sheng Ma" has been widely used in China to dissipate body heat and treat wind-heat headaches, toothaches and sore throats (Guo et al., 2017). Three species (*Cimicifuga heracleifolia* Kom., *Cimicifuga foetida* L. and *Cimicifuga dahurica* (Turcz.) Maxim) are officially listed in Chinese Pharmacopoeia 2020 and approved as additives in the functional foods (Hu et al., 2021; Qin et al., 2017). Plants within the genus *Cimicifuga* include 28 species have also been used as herbal dietary remedies in East Asia, Europe, and North America (Guo et al., 2017). Extracts from *Cimicifuga racemosa* (L.) Nutt. (Black cohosh) provide one of the best-selling herbal supplements in America and Europe for alleviating menopausal symptoms (Mohapatra et al., 2022). Previous literatures have mostly focused on purification and biological activities (including anti-osteoporosis, anti-inflammatory, anti-viral, anti-tumor, and anti-oxidant) of the organic solvent-derived extracts from "Sheng Ma", like triterpenoid saponins, phenylpropanoids, flavonoids and alkaloids (Guo et al., 2017). However, information on water-soluble oligosaccharides from "Sheng Ma" is sorely lacking.

Oligosaccharides derived from the plants have been widely used as nutrients and ingredients in the food industry (Catenza & Donkor, 2021) owing to their good water solubility, non-toxic effect, and diverse health benefits. Among these functional oligosaccharides, some of those generated from their parental polysaccharides by microbial fermentation and enzymatic or chemical degradation, including maltooligosaccharides, xylooligosaccharides and mannooligosaccharides (Moreno, Corzo, Montilla, Villamiel, & Olano, 2017). Some of these occur naturally, like the sucrose-based oligosaccharides. These include raffinose family oligosaccharides (RFOS) and fructo-oligosacchaides (FOS) that are the best known, most widespread, and widely used as functional ingredients in foods (Van den Ende, 2013). Bioactive sucrose-based oligosaccharides are found in many herbs that approved as additives in the functional foods. The RFOS are richly present in *Lycopus lucidus* Turcz., *Rehmannia glutinosa* Libosch. and *Salvia miltiorrhiza*, and possess immunomodulatory, hepatoprotective, as well as hypoglycemic and prebiotic effects (Yang, Zhao, He, & Croft, 2010; Zeng et al., 2017;

* Corresponding author.
E-mail addresses: cuiln802@nenu.edu.cn (L. Cui), wuj806@nenu.edu.cn (J. Wu), wangx004@nenu.edu.cn (X. Wang), yangxt839@nenu.edu.cn (X. Yang), yezx106@nenu.edu.cn (Z. Ye), mayox001@umn.edu (K.H. Mayo), sunl925@nenu.edu.cn (L. Sun), zhouyf383@nenu.edu.cn (Y. Zhou).

https://doi.org/10.1016/j.fochx.2023.100706
Received 10 February 2023; Received in revised form 14 April 2023; Accepted 4 May 2023
Available online 6 May 2023

Zhang, Zhou, Jia, Zhang, & Gu, 2004). The FOS, highly present in *Morinda Officinalis* How., *Arctium lappa* L., *Codonopsis pilosula* (Franch.) Nannf. and *Atractylodes lancea* (Thunb.) DC., are reported to have prebiotic, immunomodulatory, anti-diabetic, and anti-depressive activities (Bai et al., 2020; Chi et al., 2020; Yuan et al., 2021; Zhang et al., 2022).

As active components from medicinal plants, oligosaccharides might play an important role in biological activity of "Sheng Ma". To date, we have very little information on the chemical structures of oligosaccharides from "Sheng Ma", information that is crucial to understanding bioactivities from "Sheng Ma" and developing these oligosaccharides as potential pharmacological agents. Within this in mind, we have purified oligosaccharides from *Cimicifuga heracleifolia* Kom. Rhizomes and elucidated their structures in the present study. Our findings are helpful in advancing the use of *Cimicifuga heracleifolia* Kom. in the food industry.

Materials and methods

Materials and chemicals

Dried *Cimicifuga heracleifolia* Kom. rhizomes (planted in Fushun, Liaoning China) were purchased in the herbal medicine market. AB-8 macroporous resin and DEAE-Cellulose were purchased from Yuanye Bio-Technology Company Limited (Shanghai, China). Bio-gel P-4 extra fine was purchased from Bio-Rad company (Hercules, CA, USA). HPLC grade acetonitrile (ACN) and 50% (w/w) sodium hydroxide (NaOH) solution for HPAEC were purchased from ThermoFisher Scientific (Waltham, MA, USA). Anhydrous sodium acetate (NaAc) for HPAEC study was obtained from J&K Scientific Ltd (Beijing, China). Saccharide standards, including mannose (Man), glucose (Glc), galactose (Gal), fructose (Fru), rhamnose (Rha), fucose (Fuc), xylose (Xyl), arabinose (Ara), galacturonic acid (GalA), glucuronic acid (GlcA), sucrose (Suc) and dextran with different molecular weights (i.e. Mw 1 kDa, 5 kDa, 25 kDa, 50 kDa, 80 kDa), were obtained from Sigma (St. Louis, MO, USA). Inulin standard (extracted from dahlia tubers) was purchased from Aladdin Biochemical Technology Co., Ltd (Shanghai, China). All other chemicals and reagents were of analytical grade made in China.

Oligosaccharide extraction and isolation

Dried *Cimicifuga heracleifolia* Kom. rhizomes (1 kg) were cut into thick slices (2–4 mm), washed to remove dust, and extracted 3-times (3 hr each) in 16 L distilled water at 100℃. The extracted aqueous phase was filtrated and concentrated to around 2 L at 60℃ on a rotary evaporator. After centrifugation (4500 rpm for 30 min), the supernatant was precipitated by addition of 95% ethanol to a final concentration of 80%. The precipitate was re-dissolved in distilled water and lyophilized to obtain *Cimicifuga heracleifolia* Kom. rhizome-derived carbrohydrates (CRC, 150 g) (Prieto-Santiago et al., 2022; Yuan et al., 2021). The CRC (50 g) was run through an anion-exchange DEAE-cellulose column (9.8 cm × 30 cm, Cl^-), and the aqueous eluate was centrifuged (4500 rpm for 30 min) and further subjected to hollow fiber ultrafiltration membrane filter (3 kDa, Cytiva, Washington D.C., USA). The filtrate from the membrane was then applied to an AB-8 macroporous resin column (9.8 cm × 30 cm). The un-bound fraction eluted with distilled water was collected, concentrated, and lyophilized to yield the oligosaccharides (CRO, 32 g) (Liang, Liu, Yu, Song, & Li, 2019; Liu et al., 2021). The phenol–sulfuric acid method (DuBois, Gilles, Hamilton, Rebers, & Smith, 1956) was used to monitor eluate fractions during the purification process. The Seliwanoff test (Shahidullah & Khorasani, 1972) was conducted to determinate the Fru content. Protein content was determined by the Bradford method (Sedmak, & Grossber, 1977), with bovine serum albumin (BSA) as the standard. To determine the ash content (Benhura, Mbuya, & Machirori, 1999), an oligosaccharide sample (100 mg) was heated in a muffle furnace at 550℃ for 5 h until it reached a constant weight.

Separation and purification of oligosaccharide monomers in CRO

Size exclusion chromatography (SEC) purification

The CRO (3 g) was dissolved in 6 mL deionized water and centrifuged (12,000 rpm for 10 min). After filtration (0.22 μm membrane), the supernatant was loaded onto two sequential Bio-gel *P*-4 columns (5 × 100 cm each) linked to a medium pressure liquid chromatography (MPLC) system (SCG-030, Sepure Instrument Co., Ltd., Suzhou, Jiangsu, China). Columns were eluted with deionized water at a flow rate of 1.5 mL/min, and fractions were collected (15 mL/tube) and detected using a refractive index detector (RID). Fractions of the same top peak were combined, concentrated and lyophilized to obtain oligosaccharide pools with different DP values (Shi, Xu, Wang, Jia, Zhou, & Sun, 2020; Zheng et al., 2018).

Hydrophilic interaction liquid chromatography (HILIC) purification.

Oligosaccharide pools collected from SEC were dissolved in 50% ACN (50 mg/mL), filtered through a 0.22 μm membrane, and applied on to HILIC for further purification (Honda et al., 2021). Oligosaccharide samples were first analyzed on a HPLC-ELSD system (1260 Infinity II, Agilent, CA, USA) equipped with an analytical scale HILIC column (Asahipak NH2P-50 4E, 4.6 mm × 250 mm, Shodex, Tokyo, Japan) and an integrated pre-column (Asahipak NH2P-50G 4A, 4.6 mm × 10 mm, Shodex, Tokyo, Japan). Various isocratical solvent concentrations (50% to 90% [v/v] ACN) were investigated for optimal separation and preparation of oligosaccharide monomers. The column temperature was 40℃, and eluted at a flow rate of 1 mL/min. The injection volume was 10 μL; the gas flow rate was 1 SLM, and the temperature of the nebulizer and evaporator in the ELSD was 50℃ and 90℃, respectively.

Using chromatographic conditions optimized above, oligosaccharide samples (injection volume of 100 μL after filtration) were loaded onto a semi-preparative scale HILIC column (Asahipak NH2P-50 10E, 10 mm × 250 mm, Shodex, Tokyo, Japan) with an integrated pre-column (Asahipak NH2P-50G 4A, 4.6 mm × 10 mm, Shodex, Tokyo, Japan) to prepare oligosaccharide monomers. The purification was performed on a HPLC-RID system (Prominence LC-20AT, Shimadzu, Tokyo, Japan), and an isocratic elution with 67.5% (v/v) acetonitrile/water was used for preparation of oligosaccharide monomers from DP 2 to DP 9, and 62.5% (v/v) acetonitrile/water was used for DP 10 to DP 14. The column temperature was 40℃, and was eluted at a flow rate of 3 mL/min. To ensure purity of the oligosaccharide monomers, the eluate of each peak was collected partially or completely based on peak resolution.

Structural analysis of oligosaccharide monomers

Molecular weight analysis

Relative molecular weight (Mw) and distribution of samples were determined by using high performance gel-permeation chromatography (HPGPC) carried out on a HPLC-RID system (Prominence LC-20AT, Shimadzu, Tokyo, Japan) equipped with a TSK-gel G-3000 PWXL chromatography column (7.8 × 300 mm, TOSOH, Tokyo, Japan) at 35 ℃. The mobile phase was 0.2 M NaCl and the flow rate was 0.6 mL/min. Samples having concentration of 5 mg/mL were filtered through a 0.22 μm membrane before analysis, and the injection volume was 20 μL. Dextran standards with different molecular weights (Mw 1 kDa, 5 kDa, 25 kDa, 50 kDa, 80 kDa) and Glc (Mw 180 Da) were used to established the calibration curve.

Matrix-assisted laser desorption-time of flight-mass spectrometry (MALDI-TOF-MS) measurement was used to determine the molecular weight and DP value of the oligosaccharides. Samples were dissolved in distilled water (5 mg/mL). 2,5-dihydroxy benzoic acid was dissolved in a solution of 30/70 (v/v) acetonitrile/0.1% TFA as the matrix. Equal volumes of sample and matrix were mixed. The mixture (1 μL) was placed on a AnchorChip Standard (800 μm) plate and examined using a BRUKER Autoflex Speed mass spectrometer (Karlsruhe, Germany).

Monosaccharide composition analysis

Acid hydrolysis was performed to release monosaccharides in the oligosaccharide samples, and the concentration of each sample in an acidic solution was 1 mg/mL. Oligosaccharide samples were hydrolyzed under both violent (2 M TFA, 120 ℃, 1 h) and mild (0.01 M TFA, 80 ℃, 1 h) hydrolytic conditions to confirm their monosaccharide compositions because of the presence of Fru residues. Following hydrolysis, TFA in the hydrolysate was removed by addition of ethanol (three times) under streaming N_2. The hydrolysate was re-dissolved in 1 mL of deionized water and centrifuged (12000 rpm for 10 min); then the supernatant was diluted 40 times, filtered (0.22 μm membrane) and analyzed by high performance anion exchange with a pulsed amperometric detection (HPAEC-PAD) system (ThermoFisher Scientific ICS-5000$^+$, Waltham, MA, USA). The column was a CarboPac^{TM} PA20 column (3 × 150 mm, ThermoFisher Scientific, Waltham, MA, USA) in which the sample was eluted at a flow rate of 0.4 mL/min using the following protocol: −10–6 min isocratic elution with 100 mM NaOH; −5.99-0 isocratic elution with 2 mM NaOH; 0.01–30 min, isocratic elution with 2 mM NaOH; 30.01–45 min, a linear gradient from 0 to 200 mM NaAc/2 mM NaOH.

Methylation analysis

Methylation analysis was carried out according to the method of Needs and Selvendran (Needs & Selvendran, 1993). Oligosaccharide samples (2 mg each) were dissolved in dimethyl sulfoxide (DMSO, 0.5 mL) and methylated by treatment with a suspension of NaOH/DMSO (0.5 mL) and iodomethane (1 mL). The reaction mixture was extracted with $CHCl_2$, and then the solvent was removed by vacuum evaporation. Complete methylation was confirmed by the disappearance of the –OH band (3200–3400 cm^{-1}) in FT-IR spectrum using a Spectrum Two FT-IR spectrometer (Perkin Elmer, Waltham, MA, USA). The per-O-methylated oligosaccharide was hydrolyzed subsequently by using TFA (1 M, 1 mL) for 30 min at 60 °C, with addition of *tert*-butyl alcohol prior to evaporation to minimize decomposition of O-methyl fructofuranosyl derivatives (de Oliveira et al., 2011). Partially methylated sugars in the hydrolysate were reduced by using $NaBD_4$ and acetylated. The resulting partially methylated alditol acetates (PMAA) were analyzed by using gas chromatography–mass spectrometry (GC–MS, 7890B-5977B, Agilent, CA, USA) with a HP-5 ms capillary column (30 m × 0.32 mm × 0.25 mm). The oven temperature was programed as follows: the original temperature of the column was 140 °C (held for 1 min), increased by 5 °C/min to 170 °C (held for 3 min), then taken up to 180 °C (held for 5 min) at 1 °C/min, and then increased by 3 °C/min to 220 °C (held for 1 min), and then finally up to 295 °C (held for 3 min) at 20 °C/min. Both the inlet and detector temperatures were 300 °C. Helium was used as the carrier gas. The mass scan range was 50 to 500 *m/z*.

Nuclear magnetic resonance (NMR) spectroscopy

^1H, ^{13}C, HSQC and HMBC NMR spectra were recorded at 25 °C on a Bruker Avance 600 spectrometer (Bruker, Karlsruhe, Germany), operating at 600 MHz for ^1H and 150 MHz for ^{13}C NMR. Oligosaccharide samples (5 mg each) were dissolved in D_2O (99.8 %, 0.5 mL), freeze-dried, and re-dissolved in D_2O (0.5 mL). Chemical shifts are given in ppm, with acetone as the internal chemical shift reference.

HPAEC-PAD analysis

Oligosaccharide samples were dissolved in deionized water (20 μg/mL), filtered (0.22 μm membrane) and chromatographed on a CarboPac PA200 column (3 × 250 mm, ThermoFisher Scientific, Waltham, MA, USA) at 35 °C using a HPAEC-PAD system (ThermoFisher Scientific ICS-5000$^+$, Waltham, MA, USA). The column was eluted at a flow rate of 0.5 mL/min using the following protocol: −5–0 min, isocratic elution with 10 mM NaAc/100 mM NaOH; 0.01–20 min, a linear gradient from 10 to 350 mM NaAc/100 mM NaOH; 20.01–30 min, isocratic elution with 500 mM NaAc/200 mM NaOH.

Quantification analysis of oligosaccharide monomers in CRO by HPAEC-PAD

Standard solutions and sample preparation

Sucrose- and inulin-type FOS monomers (DP 3–13) were weighed accurately to prepare standard stock solution A in deionized water with a concentration of 25 μM/L. Similarly, standard stock solution B (25 μM/L) was prepared using inulo-*n*-ose-type FOS monomers (DP 2–13). CRO were weighed accurately and dissolved in deionized water at a concentration of 5 mg/L for further quantitative analysis. The process of HPAEC-PAD analyses was same as stated in the previous section.

Method validation

HPAEC-PAD quantitative analysis was performed using a calibration curve, limit of detection (LOD) and limit of quantification (LOQ) for each analyte. Standard stock solutions A and B were diluted with deionized water to prepare twelve concentrations of mixed standard solutions and analyzed in triplicate to construct calibration curves. The linear range and regression analysis were determined, and the regression coefficient (R^2) was calculated for each calibration curve. The limit of detection (LOD) and limit of quantification (LOQ) for each analyte were determined by using mixed standard solutions with appropriate concentrations at a signal-to-noise (S/N) of about 3 and 10, respectively.

The precision, repeatability, stability and accuracy of the method were also investigated. The relative standard deviation (RSD%) of peak area and retention times for intra-day and inter-day measurements of the mixed standard solutions (0.5 μM/L) were calculated to evaluate the precision of the HPAEC-PAD method. For the intra-day precision test, mixed standard solutions were analyzed in six replicates within one day, whereas for the inter-day precision test, solutions were examined in duplicate on three consecutive days. The reproducibility of the HPAEC-PAD method was determined by analysis of six parallel samples at the test concentration (0.5 μM/L). Stability was tested and analyzed at 0, 1, 2, 4, 8, 12 and 24 h. Recovery experiments were conducted to evaluate the accuracy of the HPAEC-PAD method, with the protocol for recovery experiments as follows: accurate amount of mixed standards were spiked into the sample, then the mixture was processed and quantified based on the method mentioned above. Average recoveries were expressed by the equation: recovery (%) = 100 × (observed amount − original amount)/spiked amount. Results of reproducibility, stability and accuracy were expressed as RSD% of integrated areas under peaks.

Results

Extraction and isolation of CRO from Cimicifuga heracleifolia Kom. rhizomes

The protocol used for extraction and isolation of CRO is shown as a flow chart in **Fig. S1**. CRC was obtained by sequential hot-water extractions and ethanol precipitations from dried *Cimicifuga heracleifolia* Kom. rhizomes. HPGPC analysis (Fig. S2**A**) showed that oligosaccharides (Mw < 3 kDa, retention time >13.9 min) were the main components in CRC. Anion-exchange chromatography, hollow fiber membrane ultrafiltration (3 kDa molecular weight cutoff) and macroporous resin adsorption chromatography were combined to isolate CRO from CRC. This approach aimed to remove impurities, including polysaccharides, pigments, charged amino acids, and other small molecules.

The CRO yield relative to *Cimicifuga heracleifolia* Kom. rhizomes was about 9.5%. CRO molecular weight was <3 kDa, and its distribution from HPGPC was narrower than that of CRC (Fig. S2**A**). The DP distribution of CRO in MALDI-TOF spectrum (Fig. S2**B**) ranged from 2 to 18. Seliwanoff test results suggested that fructo-oligosaccharides (FOS) are predominant in CRO, with the fructose content being about 84% (w/w). In addition, CRO also contained ~5% ash and little protein (~1.5%). Because it is a ketose, fructose in CRO is more susceptible to acid than other monosaccharides and therefore easier to be released. Significantly,

released fructose is degraded to non-sugars under violent hydrolytic conditions (2 M TFA, 120 ℃, 1 h) that are suitable for release of other monosaccharides, leading to the inaccuracy in monosaccharide composition analysis (Dong et al., 2015). Both violent (2 M TFA, 120 ℃, 1 h) and mild (0.01 M TFA, 80 ℃, 1 h) hydrolytic conditions were conducted to detect monosaccharide compositions in CRO. Under violent hydrolytic conditions, only glucose was identified in the HPAEC profile (Fig. S2**C**), whereas fructose could not be detected due to its decomposition. Fructose and glucose were released from CRO under mild hydrolytic conditions at a molar ratio of 11:1. Taken together, CRO were composed of 91.7% fructose and 8.3% glucose, which is consistent with Seliwanoff test results.

To further determine the types of fructo-oligosaccharides (FOS) present in CRO, samples were analyzed by using HPAEC-PAD and compared with an Inulin standard (mainly containing inulin-type fructo-oligosaccharides). As shown in Fig. S2**D**, >30 peaks corresponding to different oligosaccharides appeared in the chromatogram. Some compound peaks in the CRO could be matched to oligosaccharides in inulin, whereas some compound peaks could not. This demonstrates the existence of other types of fructo-oligosaccharides (FOS) aside from inulin-type fructo-oligosaccharides.

Separation and purification of CRO oligosaccharide monomers

Preparation of oligosaccharide pools with homogenous DP values

The protocol for separating and purifying CRO oligosaccharide monomers is summarized in **Fig. S1**. CRO was first loaded onto a preparative SEC system, with the goal of obtaining pools with homogenous DP values. As shown in Fig. 1**A**, sixteen peaks could be distinguished in the SEC profile. Tubes of every top peak were collected and the fractions were named CRO 1 to CRO 16 based on increasing molecular weights. CRO 1 was not further analyzed, because of its high ash content (~50%) and low total carbohydrate content (~40%). The remaining pools were analyzed by using MALDI-TOF-MS and HPAEC. MS analysis showed that CRO 2 to CRO 16 contained FOS with relatively homogenous DP values from 2 to 16. Some minor signals representing neighboring pools were present in MS traces due to incomplete separation (**Fig. S3**). For HPAEC analysis, the elution sequence of these pools was in the order of increasing oligosaccharide size. As shown in Fig. 2, all fractions from CRO 2 to CRO 16 displayed two major peaks in HPAEC chromatograms, indicating the existence of at least two isoforms of oligosaccharides in each pool. The former isomers in each fraction were named as CRO *n*-I (n = 2–14) FOS, and the later were named as CRO *n*-II (n = 2–14) FOS. Some low intensity peaks due to overlapping neighboring pools appeared in HPAEC profiles as the DP increased. This is consistent with our MS results discussed above.

Separation of oligosaccharide isomers

To further separate oligosaccharide isomers, fractions CRO 2 to CRO 16 were applied to HILIC. An analytical HILIC column (Shodex Asahipak NH2P-50 4E) was used to optimize chromatographic conditions for isomers separation. As shown in Fig. 1**B**, two major isomers in CRO 2 to CRO 9 could be well separated within 60 min using 67.5% acetonitrile isocratic elution at a flow rate of 1 mL/min. These fractions followed an elution order based on size in HILIC. However, the 67.5% acetonitrile isocratic elution condition was unsuitable for the separation of fractions with higher molecular weights (CRO 10 to CRO 16) due to relatively long retention time, broad peaks, and possible molecular diffusion. The HILIC separation profile of CRO 10 to CRO 14 is shown in Fig. 1**C.** The 62.5% acetonitrile isocratic elution achieved the separation of two major isomeric oligosaccharides within 60 min, with some overlapping peaks. Some low intensity peaks also appeared in HILIC profiles. Isomers in CRO 15 and CRO 16 with higher molecular weights resulted from relatively poor peak resolution with 62.5% acetonitrile in HILIC (data not shown). Because of their low yields, these two fractions were not purified further. Using optimized chromatographic conditions, CRO 2 to CRO 14 were then applied to semi-preparative scale HILIC columns (Shodex Asahipak NH2P-50 10E) that contained identical packing materials with the analytical columns that led to similar separation profiles (data not shown). Separated peaks were obtained with CRO 2 to CRO 9, and overlapped peaks from CRO 10 to CRO 14 were partially collected (with overlapping areas being discarded) to ensure the purity of oligosaccharide monomers. Two major isomeric oligosaccharides in each of the above fractions were isolated yielding 26 different oligosaccharide monomers.

As shown in Fig. 3, all oligosaccharide monomers showed a major homogenous peak in HPAEC with purities >95% (calculated by area normalization). DPs of these oligosaccharide monomers were also characterized by MALDI-TOF-MS (data not shown), with size and elution times listed in **Table S1**. Significantly, the elution order of the two isomers in HILIC ran contrary to that observed in HPAEC. CRO *n*-I (n = 2–14) FOS had longer retention times than CRO *n*-II (n = 2–14) FOS from HILIC. It is worth noting that CRO *n*-I (n = 2–14) FOS peaks corresponded to oligosaccharides from Inulin, demonstrating that CRO *n*-I (n = 2–14) FOS are also present in inulin-type FOS. The successful separation of almost all oligosaccharide monomers (especially isomeric oligosaccharides) in CRO was determined by combination of preparative SEC and HILIC. Structural features of the two FOS series were further analyzed.

Structural analysis of oligosaccharide monomers prepared from CRO

Structural analysis of oligosaccharides CRO 4-I and CRO 4-II

Oligosaccharides CRO 4-I and CRO 4-II were chosen for comprehensive structural analysis. Monosaccharide composition, methylation, and 1D/2D NMR analyses were combined for insight into their chemical structures. HPAEC results (**Fig. S4**) showed that the CRO 4-I hydrolysate contained Fru and Glc in a ratio of 2.6:1, indicating that CRO 4-I is composed of three Fru units and one Glc unit. The proportion of Fru in the CRO 4-I hydrolysate was <75%, due most likely to decomposition. Unlike CRO 4-I, only Fru was detected in CRO 4-II, proving that CRO 4-II is composed of four Fru units.

Methylation analysis provided glycosidic linkage information (**Table S2**). The total ion chromatograms (TICs) of partially methylated alditol acetates (PMAAs) from CRO 4-I and CRO 4-II are shown in Fig. S5**A** and **Fig. S6A**. The instability of partially methylated Fru due to acid hydrolysis, complex formation of D-mannitol and D-glucitol derivatives from partially methylated, reduced Fru, and unknown factors for all PMAAs make methylation analysis more qualitative than quantitative (de Oliveira et al., 2011; Sims, Carnachan, Bell, & Hinkley, 2018). Results showed that CRO 4-I contains 2-linked Fru*f*, 1,2-linked Fru*f* and 1-linked Glc*p*, CRO 4-II contains 2-linked Fru*f*, 1,2-linked Fru*f* and 1-linked Fru*p*. Because PMAAs from 1,2-linked Fru*f* and 2,6-linked Fru*f* co-eluted in GC–MS, labelling of anomeric carbon with deuterium (reduction with $NaBD_4$) was performed to detect differences in their mass fragmentation patterns. The selected region (containing 1,2,5-tri-O-acetyl-3,4,6-tri-O-methyl-D-mannitol/glucitol or 2,5,6-tri-O-acetyl-1,3,4-tri-O-methyl -D-mannitol/glucitol 21.193 min) of TICs and extracted ion chromatograms (EICs) are shown in Fig. S5**B-5C, S6B-6C**. Typical primary fragmentation ions for 1,2-linked Fru*f* (including *m/z* 190 and 161) were primarily detected, whereas insignificant *m/z* 189 and 162 ions (which represent 2,6-linked Fru*f*) were detected, and the low proportion of *m/z* 189 (of % *m/z* 190) and *m/z* 162 (of % *m/z* 161) might arise from the natural abundance of ^{13}C (de Oliveira et al., 2011). These results indicated that both CRO 4-I and CRO 4-II contain 1,2-linked Fru*f*, but not 2,6-linked Fru*f*. The GC–MS fragmentation ion pattern of PMAA from CRO 4-I and CRO 4-II are showed in **Fig. S7**.

NMR spectra (^1H, ^{13}C, DEPT 45°, HSQC, HMBC and TOCSY) were acquired to assess the chemical structure of CRO 4-I and CRO 4-II. In the ^1H NMR spectrum of CRO 4-I (Fig. 4**A**), only one anomeric proton signal at 5.38 ppm could be found and assigned to a α-D-Glc*p* group (residue **A**) consistent with published chemical shifts (Yang, Hu, & Zhao, 2011).

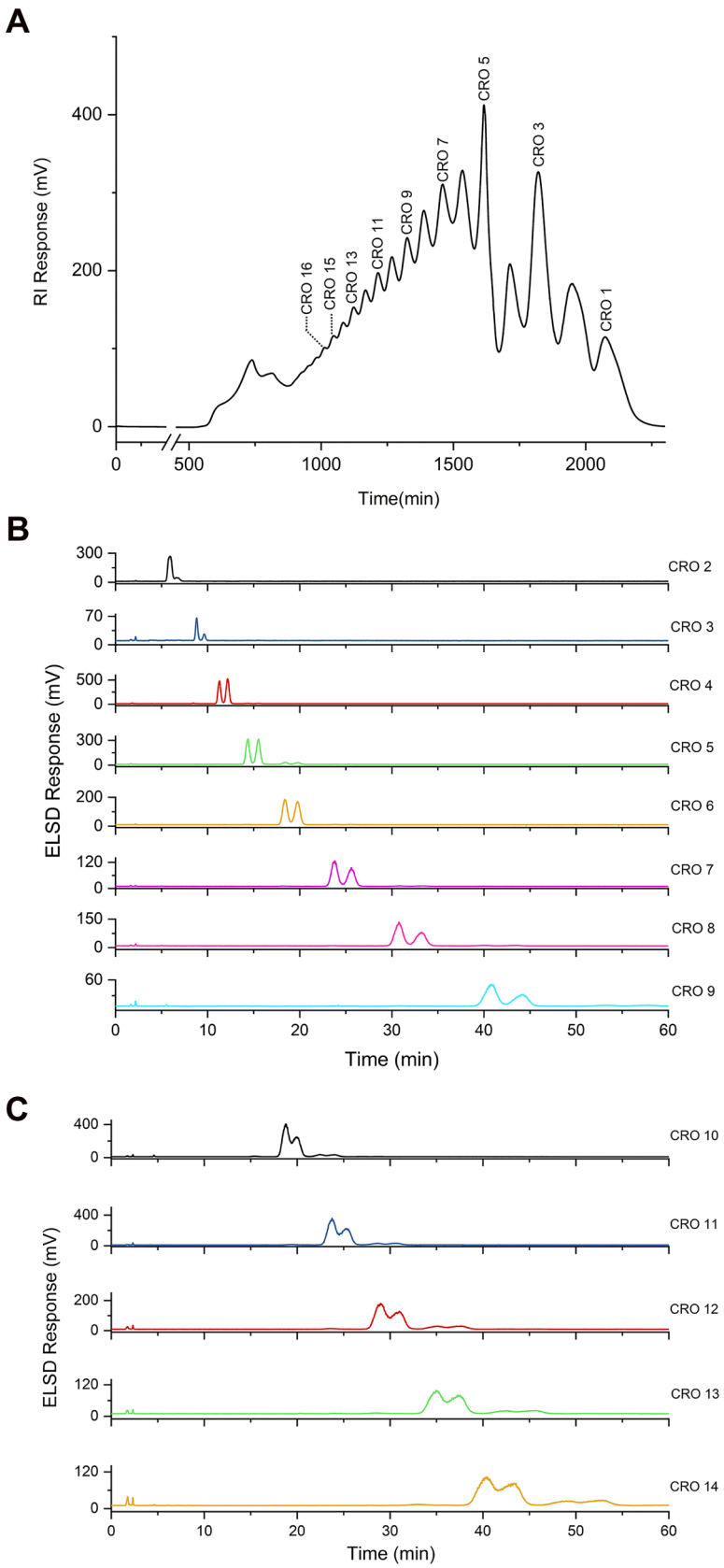

Fig. 1. (A) MPLC (SEC) -RID chromatography of CRO; HILIC (analytical scale) -ELSD chromatography of oligosaccharide pools with homogenous DP from CRO after SEC purification (B) (CRO 2–9); (C) (CRO 10–14).

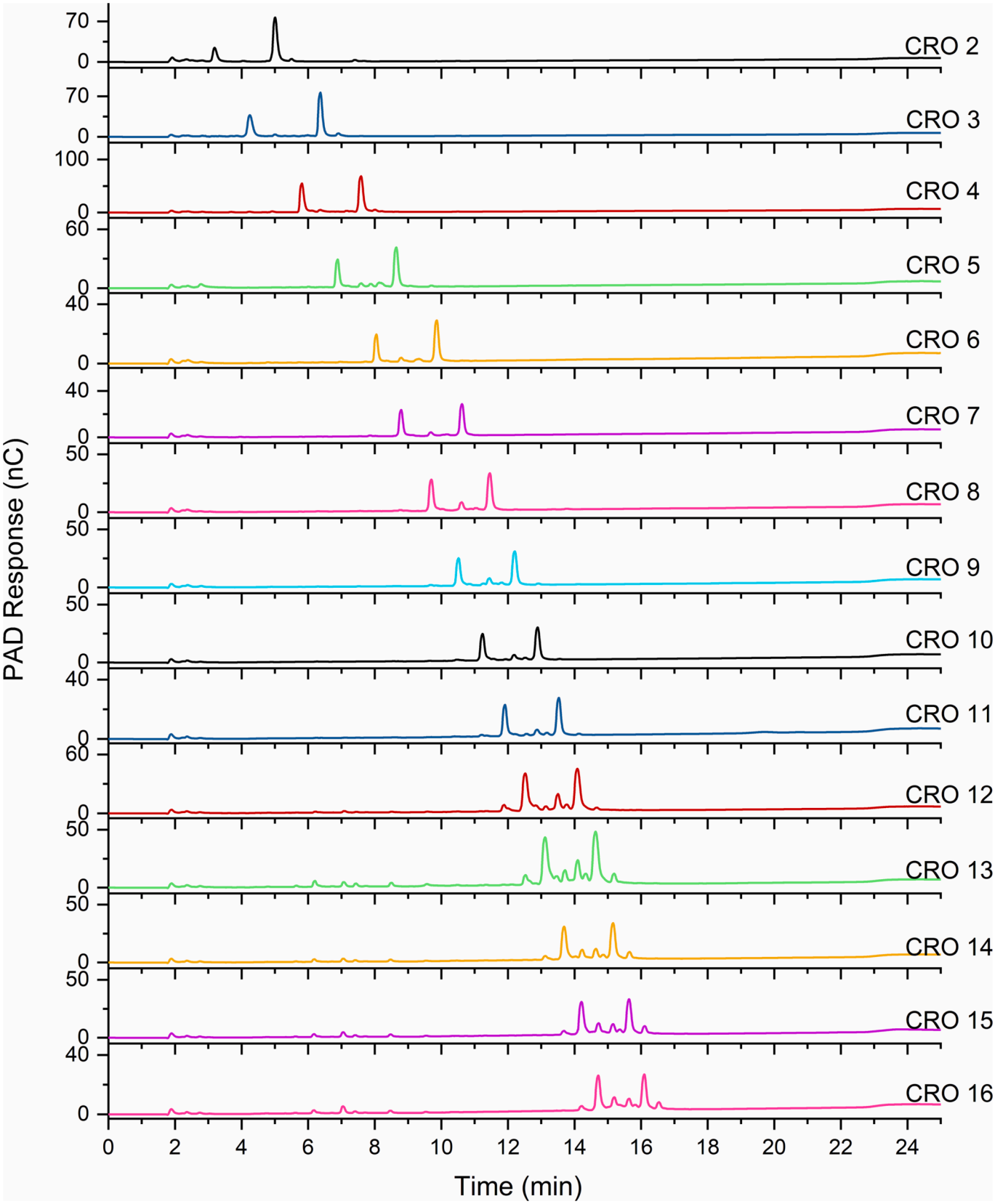

Fig. 2. HPAEC-PAD analysis of oligosaccharide pools with homogenous DP from CRO after SEC purification.

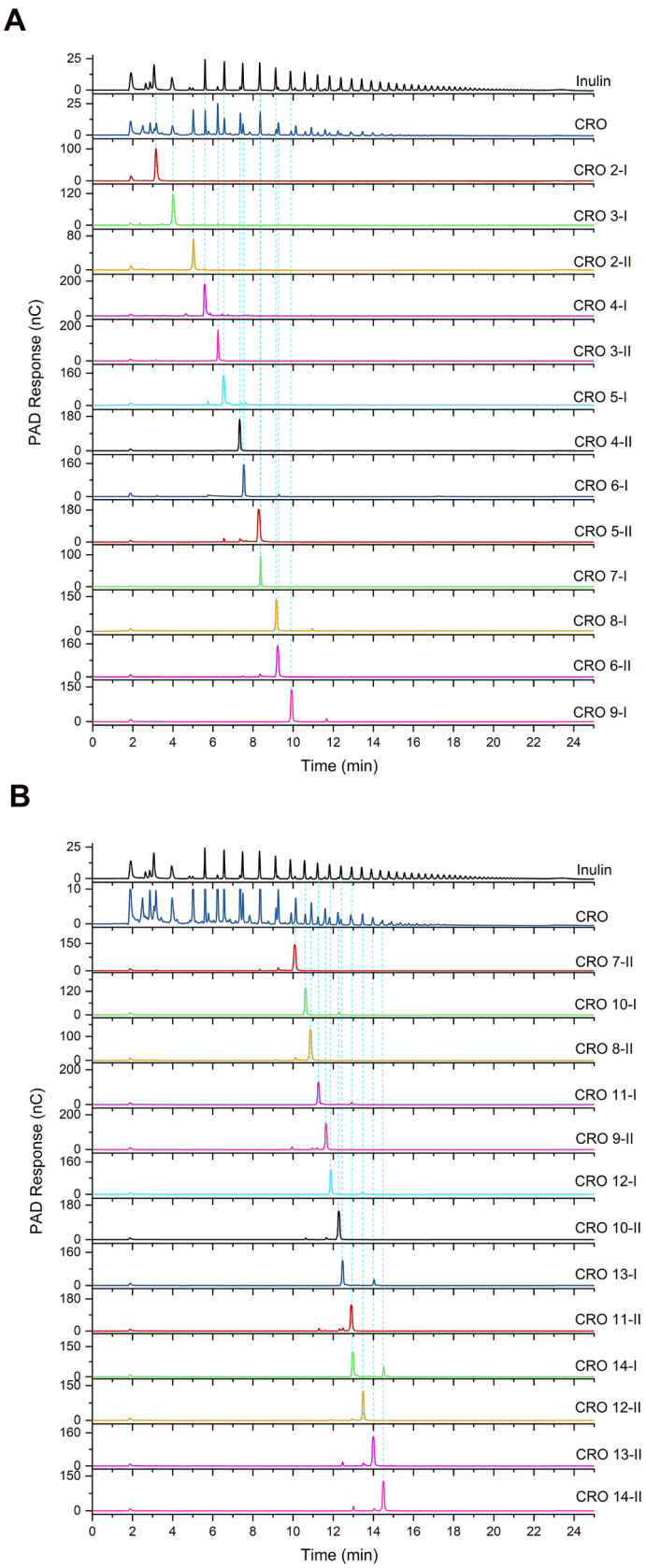

Fig. 3. HPAEC-PAD analysis of oligosaccharide monomers purified from CRO.

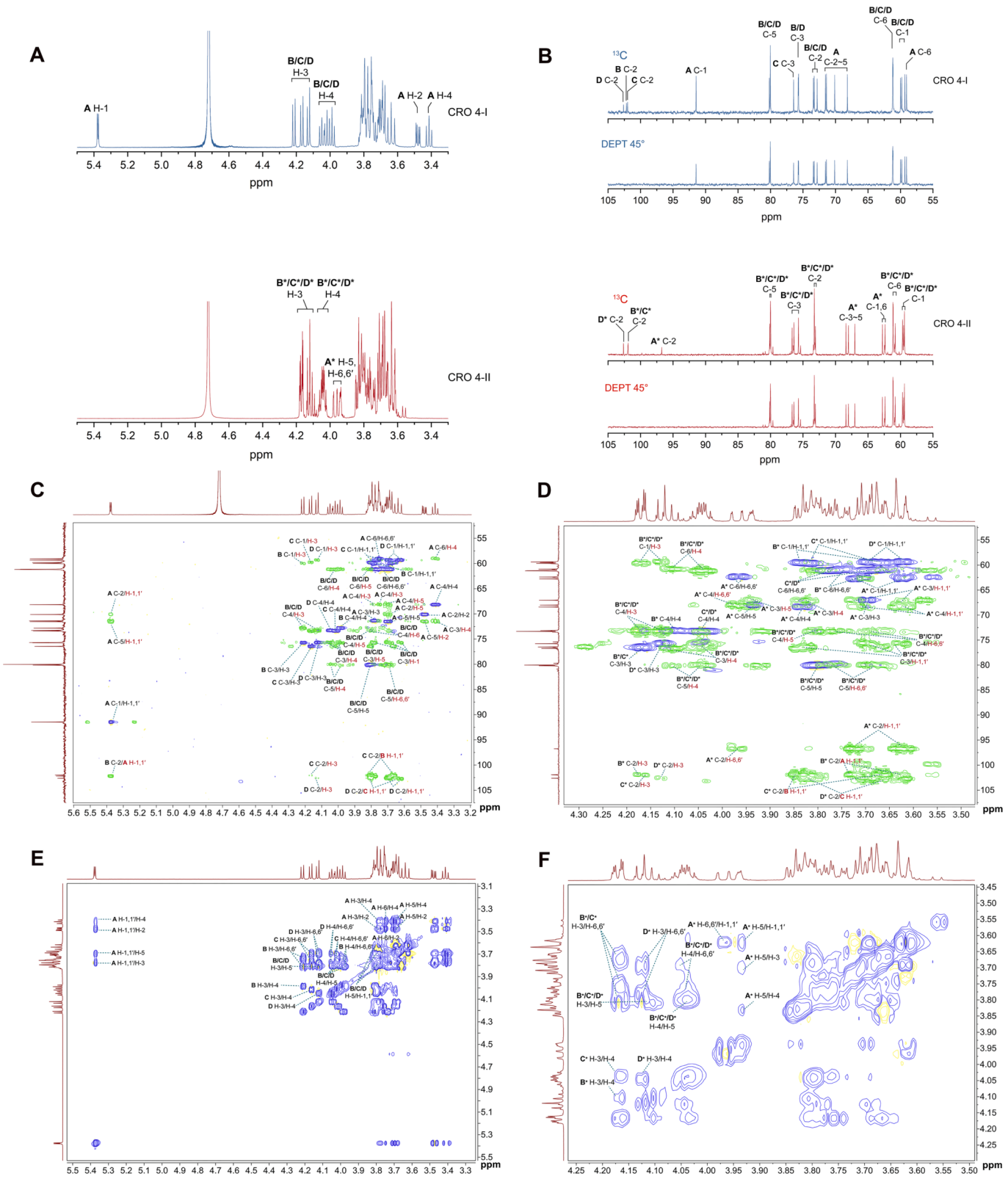

Fig. 4. (A) ^{1}H NMR spectra of CRO 4-I and CRO 4-II; (B) ^{13}C NMR and DEPT 45° spectra of CRO 4-I and CRO 4-II; (C) HSQC (blue) and HMBC (green) spectra of CRO 4-I; (D) HSQC (blue) and HMBC (green) spectra of CRO 4-II; (E) TOCSY spectrum of CRO 4-I; (F) TOCSY spectrum of CRO 4-II. (For interpretation of the references to colour in this figure legend, the reader is referred to the web version of this article.)

Signals with typical chemical shifts at 4.12 to 4.22 ppm (three distinct doublets) and 3.91 to 4.06 ppm (three overlapping triplets) could be readily assigned to H-3 and H-4 of the three β-D-Fru*f* residues in different chemical environments (He, Yan, Yao, Chen, Li, Wu, et al., 2021). The integration ratio between H-1 of α-D-Glc*p* residue and H-3(4) of β-D-Fru*f* residues indicate that CRO 4-I is composed of Fru and Glc in a ratio of 3:1, which was identical to our monosaccharide composition analysis. As shown in the ^{13}C NMR spectrum of CRO 4-I (Fig. 4**B**), the anomeric carbon signal at 91.46 ppm could be assigned to an α-D-*t*-Glc*p* unit (residue **A**) and supported by HSQC spectra (cross peak **A** C-1/H-1). The other three typical anomeric carbon signals at 101.99 ppm, 102.17 ppm and 102.62 ppm in the ^{13}C NMR spectrum were assigned to anomeric C-2 (quaternary carbon) of β-D-1,2-Fru*f*/β-D-*t*-Fru*f* residues. These groups could not be observed in the DEPT 45° spectrum (Fig. 4**B**) (Bai, Zhang, Jia, Fan, Hou, Wang, et al., 2020). Upfield carbon resonances at 80.02–80.18 ppm, 75.69–76.44 ppm, and 72.82–73.40 ppm were attributed to C-5, C-3 and C-4 of β-D-1,2-Fru*f*/β-D-*t*-Fru*f* residues, respectively. Signals at 70.12 ppm, 71.39 ppm, 68.16 ppm, 71.54 ppm and 59.06 ppm are characteristic of α-D-*t*-Glc*p* residues. Signals at 59.06-61.18 ppm were assigned to carbons of the methylene group (C1/C6) in β-D-1,2-Fru*f*/β-D-*t*-Fru*f* residues. Compared to the chemical shift (59.34 ppm) of C-1 in a β-D-*t*-Fru*f* unit (residue **D**), the diagnostic resonance in down-field carbons at 59.81 ppm and 59.99 ppm can be ascribed to two different β-D-1,2-Fru*f* residues (residues **B and C**) (Yang, Hu, & Zhao, 2011). Glycosidic correlations, such as **B** C-2/**A** H-1, **C** C-2/**B** H-1(1′) and **D** C-2/**C** H-1(1′) in HMBC spectrum (Fig. 4**C**), were observed, suggesting linkage patterns and sequences of residue **A** (α-D-*t*-Glc*p*), residue **B** (β-D-1,2-Fru*f* residue adjacent to α-D-*t*-Glc*p*), residue **C** (β-D-1,2-Fru*f* residue adjacent to β-D-*t*-Fru*f*) and residue **D** (β-D-*t*-Fru*f*) in CRO 4–1. Inter-residue cross-peaks, such as **B** C-2/H-1 (1′), **C** C-1/H-3, **B** C-3/H-4, **C** C-4/H-5 and **D** C-5/H-6 (6′) in the HMBC spectrum, helped us to distinguish β-D-Fru*f* similar residues in CRO 4-I. In addition, HSQC (Fig. 4**C**) and TOCSY (Fig. 4**E**) spectra revealed proton and carbon signals of each residue in CRO 4-I, as summarized in **Table S3**. Based on monosaccharide composition, methylation and NMR analyses, CRO 4-I is proposed to be β-D-Fru*f*-(2 → 1)-β-D-Fru*f*-(2 → 1)-β-D-Fru*f*-(2 ↔ 1)-α-D-Glc*p* (nystose).

As shown in Fig. 4**A**, resonance peaks could not be observed in the anomeric region (4.3 to 5.8 ppm) of ^{1}H NMR spectra, indicating that α-D-Glc*p* residues are most likely absent in CRO 4-II. Typical signals for H-3 and H-4 of β-D-Fru*f*, however, were observed at 4.02–4.18 ppm, which were more complex than those from CRO 4-I (He, Yan, Yao, Chen, Li, Wu, et al., 2021). In the ^{13}C NMR spectrum (Fig. 4**B**) of CRO 4–2, four anomeric signals could be distinguished, including two signals (101.95 and 101.92 ppm) for C-2 of β-D-1,2-Fru*f* residues (residues **B' and C'**), one signal (102.62 ppm) for C-2 of β-D-*t*-Fru*f* residue (residues **D'**), and an unknown signal at 96.74 ppm compared to CRO 4-I (Yang, Hu, & Zhao, 2011). In addition, this unknown anomeric carbon signal vanished in the DEPT 45° NMR spectrum (Fig. 4**B**), and could be ascribed to C-2 of fructose. Hence, it appears that CRO 4-II is composed of four fructose residues, consistent with its monosaccharide composition. According to published literature (Fujishima, Furuyama, Ishihiro, Onodera, Fukushi, Benkeblia, et al., 2009; Shiomi & Onodera, 1990), the carbon signal at 96.74 ppm belongs to C-2 of a reducing fructopyranosyl residue (Residue **A'**). Other typical signals such as **A'** C-1 (62.78 ppm) C-3 (67.03 ppm), C-4 (68.38 ppm) and C-5 (68.01 ppm) in the ^{13}C NMR spectrum, as well as cross peaks (**A'** C-2/ H-6,6′) in the HMBC spectrum (Fig. 4**D**), demonstrate the presence of β-D-1-Fru*p* (Residue **A'**). Glycosidic correlations, such as **B'** C-1/**A'** H-1, **C'** C-2/**B'** H-1 (1′) and **D'** C-2/**C'** H-1 (1′) in the HMBC spectrum, were observed, suggesting the linkage pattern and sequence of residue **A'** (β-D-1-Fru*p*), residue **B'** (β-D-1,2-Fru*f* residue adjacent to β-D-1-Fru*p*), residue **C'** (β-D-1,2-Fru*f* residue adjacent to β-D-*t*-Fru*f*) and residue **D'** (β-D-*t*-Fru*f*) in CRO 4–2. Inter-residue cross-peaks, such as **B'** C-2/H-1 (1′), **C'** C-2/H-1 (1′) and **D'** C-2/H-3 in HMBC spectrum, helped to distinguish β-D-Fru*f* in CRO 4-II. HSQC (Fig. 4**D**) and TOCSY (Fig. 4**F**) spectra allowed us to assign proton and carbon signals of each residue in CRO 4-II, as summarized in **Table S4**. Based on monosaccharide composition, methylation and NMR analyses results, CRO 4–2 appears to be β-D-Fru*f*-(2 → 1)-β-D-Fru*f*-(2 → 1)-β-D-Fru*f*-(2 → 1)-β-D-Fru*p* (inulotetraose).

^{13}C NMR analysis of oligosaccharide monomers

Based on the residues in CRO 4-I and CRO 4-II, we inferred that CRO *n*-I FOS are inulin-type, whereas CRO *n*-II FOS are inulo-*n*-ose-type. To verify the above deductions, ^{13}C NMR analyses of all oligosaccharide monomers prepared from CRO were performed. ^{13}C NMR spectra of partial oligosaccharides are shown in Fig. 5, including CRO *n*-I (n = 4, 6, 8, 10, 12, 14) and CRO *n*-II (n = 3, 5, 7, 9, 11, 13) FOS. For CRO *n*-I FOS, three types of anomeric carbon signals were readily identified (Fig. 5**A**). Peaks at 102.61–102.64 ppm, 91.42–91.45 ppm could be attributed to the anomeric carbons of β-D-*t*-Fru*f* and α-D-*t*-Glc*p* residues, respectively. Peaks at 101.98–102.04 ppm became overlapped as the DP of oligosaccharides increased, but could be assigned to anomeric carbons of repeating β-D-1,2-Fru*f* residues. Distinct signals at 70.12–70.13 ppm, 71.54–71.55 ppm, 68.16–68.17 ppm, 71.38–71.39 ppm and 59.05–59.07 ppm were attributed to C-2-C-6 of α-D-*t*-Glc*p* residues. Peak signals at 59.33–59.43 ppm, 75.69–75.71 ppm, 73.28–73.29 ppm, 80.01–80.03 ppm and 61.06–61.22 ppm were assigned to C-1, C-3, C-4, C-5 and C-6 of β-D-*t*-Fru*f* residues. Major overlapping carbon signals at 59.65–59.97 ppm, 75.90–76.44 ppm, 72.80–73.39 ppm, 80.02–80.18 ppm and 61.06–61.23 ppm were ascribed to C-1, C-3, C-4, C-5 and C-6 of β-D-1,2-Fru*f* residues (Bai et al., 2020; He et al., 2021; Yang, Hu, & Zhao, 2011). While the intensities of carbon signals belonging to β-D-*t*-Fru*f* and α-D-*t*-Glc*p* residues decreased with the increasing DP of oligosaccharides, the intensities of carbon signals belonging to β-D-1,2-Fru*f* residues increased, indicating higher proportion. The remaining other CRO *n*-I oligosaccharides showed similar ^{13}C NMR spectra with the above oligosaccharides (data not shown). We deduced that CRO *n*-I FOS are inulin-type FOS, except for CRO 2-I being sucrose, consistent with HPAEC results. CRO *n*-I FOS contain an increasing number of β-D-1,2-Fru*f* units attached to a terminal glucose. The chemical structure (**Fig. S8A**) and formula of these could be characterized as β-D-Fru*f*-(2 → 1)-[β-D-Fru*f*-(2 ↔ 1)]$_{n=1\text{-}12}$-α-D-Glc*p*, meaning CRO 3-I was 1-ketose (GF_2), CRO 4-I was Nystose (GF_3), CRO 5-I (GF_4) was 1,1,1-kestopentaose, etc (G as glucose, F as fructose and n as the number of internal fructose unit).

In ^{13}C NMR spectra of CRO *n*-II FOS (Fig. 5**B**), carbon signals of β-D-*t*-Fru*f* and β-D-1,2-Fru*f* residues were distinguished compared to CRO n-1 FOS. Signals at 59.36–59.42 ppm, 102.58–102.64 ppm, 75.70–75.72 ppm, 73.20–73.31 ppm, 80.00–80.03 ppm and 61.07–61.19 ppm correspond to C1-C6 of β-D-*t*-Fru*f* residues. With the increasing DP of oligosaccharides, overlapping signals at 59.45–59.83 ppm, 101.93–102.18 ppm, 75.92–76.59 ppm, 73.09–73.31 ppm, 80.00–80.15 ppm and 60.80–61.19 ppm were attributed to C1-C6 having an increasing number of β-D-1,2-Fru*f* units with greater intensities compared with β-D-*t*-Fru*f* residues (Yang, Hu, & Zhao, 2011). Unlike CRO *n*-I FOS, signals attributed to α-D-*t*-Glc*p* residues could not be found in spectra of CRO *n*-II FOS, indicating the absence of α-D-*t*-Glc*p* residues. An anomeric carbon signal appeared at lower field around 96.74–96.75 ppm, with its intensity decreasing with increasing DP values. Based on published literature (Fujishima et al., 2009; Shiomi & Onodera, 1990), we assigned C-2 of β-D-1-Fru*p* residues. Other five distinct peaks were ascribed to C-1 (62.77–62.78 ppm), C-3 (67.02–67.04 ppm), C-4 (68.38–68.39 ppm), C-5 (68.01–68.02 ppm) and C-6 (62.38–62.40 ppm) of β-D-1-Fru*p* residues. We then deduced that CRO *n*-II FOS contain an increasing number of β-D-1,2-Fru*f* units attached to a reducing fructopyranosyl residue at the terminus, making them inulo-*n*-ose-type FOS. The chemical structure (**Fig. S8B**) and formula of these species could be characterized as β-D-Fru*f*-(2 → 1)-[β-D-Fru*f*-(2 → 1)]$_{m=0\text{-}12}$-β-D-Fru*p*, indicating that CRO 2-II is an inulobiose (F_2), CRO 3-II is an inulotriose (F_3), CRO 4-II is an inulotetraose (F_4), etc. Here, F stands for fructose and m is the number of internal fructose units.

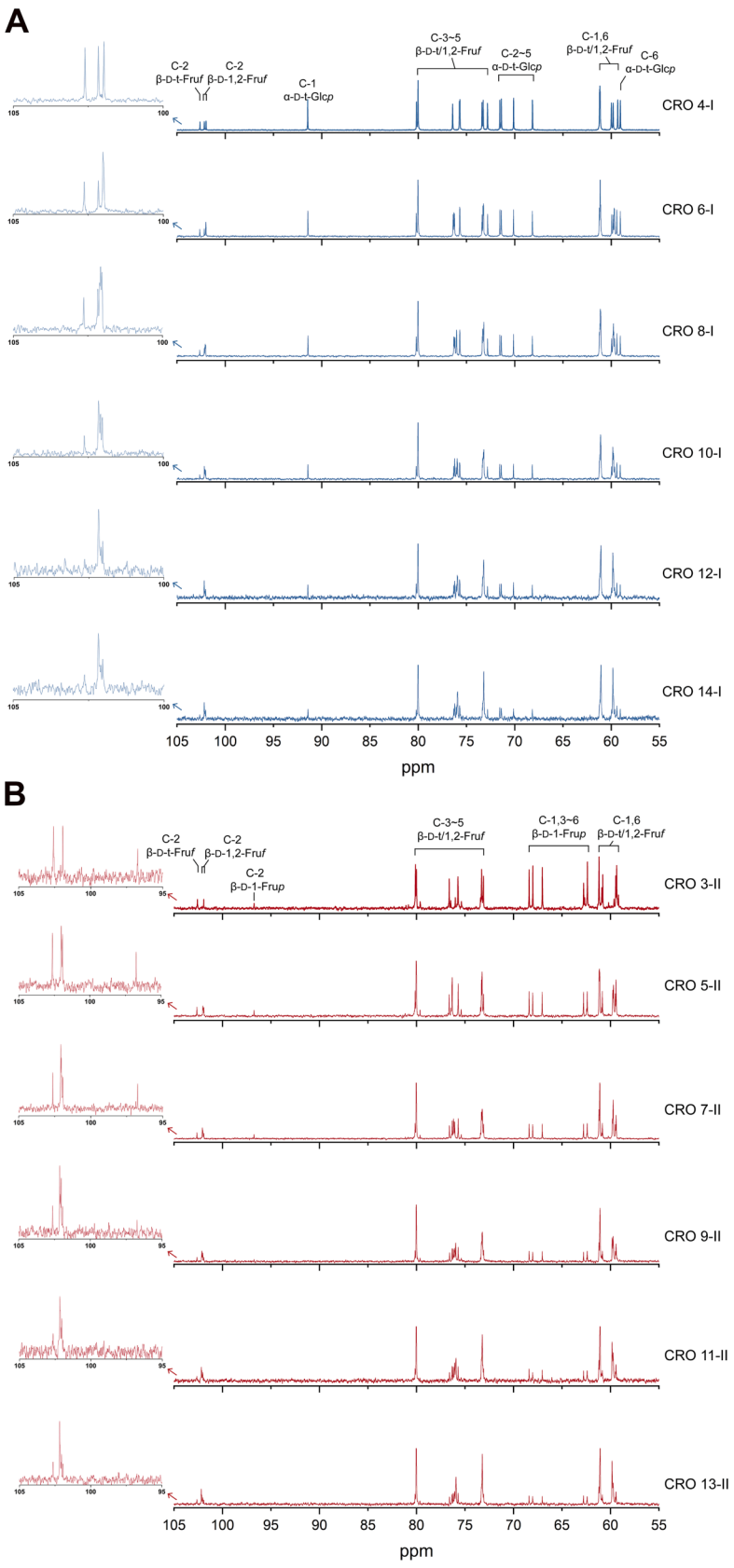

Fig. 5. (A) ^{13}C NMR spectra of partial CRO *n*-I series FOS monomers; (B) ^{13}C NMR spectra of partial CRO *n*-II series FOS monomers.

Quantification of FOS in CRO

For qualitative and quantitative analysis of FOS, HPAEC is reported to be superior to HILIC in baseline separation and analytical range of FOS with higher DP values (Pöhnl, Böttcher, Schulz, Stürtz, Widder, Carle, et al., 2017). Hence, we used the HPAEC-PAD method to quantify FOS in CRO. For this, we used the 26 oligosaccharide monomers prepared above as reference compounds. To validate the HPAEC-PAD method, we determined the linearity, regression equation, and linear ranges of the 26 oligosaccharide monomers (**Table S1**). Because some oligosaccharides, such as CRO 5–2 and CRO 7–1, CRO 12–2 and CRO 15–1, CRO 11–2 and CRO 14–1, CRO 13–2 and CRO 16–1, could not be separated completely by HPAEC, inulin-type FOS (containing sucrose) and inulo-*n*-ose-type FOS standards were analyzed independently.

Our results indicated that all standards have good linearity ($R^2 >$ 0.99874) using analytical concentrations. Slopes of calibration curves were between 0.2453 and 2.5632, and their LODs and LOQs ranged from 0.0028 to 0.0125 μM/L and 0.0083–0.0625 μM/L, respectively. Precision, reproducibility, stability and accuracy of the HPAEC-PAD method were further validated (**Table S5**). The intra-day precision of peak area (RSDs < 1.5%) and retention time (RSDs < 0.3%) were very good for all compounds. For inter-day precision, RSDs increased as expected. RSDs of peak area and retention time were below 1.8% and 0.4%, respectively. Reproducibilities of oligosaccharide monomers detected were < 1.7%. Recoveries ranged from 97.7% to 102.6% for most of analytes.

The contents (w/w) of the two FOS series in CRO were calculated based on individual calibration curves, except for some incomplete separation of oligosaccharides (CRO 7-I, CRO 5-II, CRO 11-II, CRO 12-II, CRO 13-II, CRO 14-I) and oligosaccharides with high DP > 14). Quantification showed that the contents of inulin-type FOS ranged from 1.1% to 13.3%, and contents of inulo-*n*-ose-type FOS monomers ranged from 0.7% to 5.1%. GF_2 possessed the highest content (13.3%), with the content of GF_2-GF_8 (3.1%-13.3%) being significantly higher than those of GF_9-GF_{13} (1.1%-2.2%). Content differences of F_2-F_{10} (3.2%-5.1%) were insignificant. The total content of inulin-type FOS was generally equal to that of inulo-*n*-ose-type FOS.

Discussion

FOS are usually extracted from the inulin-rich plant materials or prepared from inulin by *endo*-inulinase hydrolysis. These species primarily contain a mixture of inulin-type and inulo-*n*-ose-type FOS in different proportions (Singh, Singh, & Kennedy, 2016). Inulo-*n*-ose-type FOS can be generated from inulin and inulin-type FOS by *endo*-inulinase hydrolysis, as well as being synthesized in plants by fructan:fructan fructosyltransferase (FFT) using Fru as an acceptor (Ishiguro, Ueno, Onodera, Benkeblia, & Shiomi, 2011). The identification of these two different types FOS and their quantitation are challenging due to the unavailability of inulo-*n*-ose-type FOS standards that has hindered analysis of FOS used in food products. Inulin-type FOS monomers with a wide DP range (DP 2–18) have been prepared from inulin-rich plants (Zhang, Zhuang, Wang, Liu, Lv, & Meng, 2022). However, few reports have focused on preparation of inulo-*n*-ose-type FOS monomers, and at this point, only inulo-*n*-ose-type FOS monomers with DP values of 2–5 have been reported (Fujishima et al., 2009; Ronkart et al., 2007). Inulo-*n*-ose-type FOS monomers (DP 6–14) purified from *Cimicifuga heracleifolia* Kom. have increased the number of inulo-*n*-ose-type FOS standards, that make it possible to identify and quantity them. The HPAEC elution order of inulin- and inulo-*n*-ose-type FOS have already been summarized using a limited number of actual standards (Pöhnl et al., 2017), whereas the elution orders of two different types FOS in HILIC are ambiguous. Our results demonstrate that the HILIC elution order of inulin- and inulo-*n*-ose-type FOS isomers run contrary to those from HPAEC, an observation that is significant for the identification and purification of FOS.

Based on published literature, FOS from other herbs, such as *Morinda Officinalis* How., *Arctium lappa* L., *Codonopsis pilosula* (Franch.) Nannf. and *Atractylodes lancea* (Thunb.) DC., have been identified as inulin-type FOS with different DP ranges (Bai et al., 2020; Yang, Hu, & Zhao, 2011; Yuan et al., 2021; Zhang et al., 2022). Unlike these herbs, *Cimicifuga heracleifolia* Kom. was found to contain both inulin- and inulo-*n*-ose-type FOS with similar total content. One can speculate that the biological activities of CRO may be different from those of FOS in the above herbs. The DP and structural composition of FOS play a crucial role in their biological activities. Inulin-type FOS with low DP have been reported to exhibit better prebiotic, antioxidant and immunomodulatory activities than those with high DP (Zhang et al., 2022). The higher ratio of GF_2-GF_8 in CRO might be contributable to its bioactivities. Previous studies showed that inulin-type FOS (DP 2–4) have better capacities to promote the growth of *Bifidobacterium* than an inulin- and inulo-*n*-ose-type FOS mixture (DP 3–6) (Wang, Pan, Zhang, & Yan, 2020), indicating that these two different types FOS might possess distinct functions. Structure-activity relationships of inulo-*n*-ose-type FOS are rarely studied and remain essentially unknown owing to their limited availability. How does the DP affect the biological activities of inulo-*n*-ose-type FOS? What are the differences between the function of inulo-*n*-ose- and inulin-type FOS isomers? Do synergistic or antagonistic effects exist between these two types of FOS when they have biological impact? Questions like these remain to be answered, and further research should focus on the functions of CRO and structure–activity relationships of these different types of FOS.

Conclusions

In summary, *Cimicifuga heracleifolia* Kom. oligosaccharides (CRO) have been isolated and characterized for the first time. Twenty-six oligosaccharide monomers, including sucrose, inulin-type FOS {β-D-Fru*f*-(2 → 1)-[β-D-Fru*f*-(2 ↔ 1)]$_{n=1\text{-}12}$-α-D-Glc*p*; DP 3–14}, and inulo-*n*-ose-type FOS {β-D-Fru*f*-(2 → 1)-[β-D-Fru*f*-(2 → 1)]$_{m=0\text{-}12}$-β-D-Fru*p*; DP 2–14} have been purified from CRO and their chemical structures have been identified. The CRO was found to be composed of inulin- and inulo-*n*-ose-type FOS with similar total content. Inulo-*n*-ose-type oligosaccharides with DP 6–14 were first reported to be purified from plants. Authentic standard, preparation strategy, structural information, chromatography retention behavior and quantitation method for these different types of FOS are provided. Our findings give important information on oligosaccharides from *Cimicifuga heracleifolia* Kom. that will allow for further functional evaluation and food applications, as well as to contribute to the identification and characterization of FOS in food products.

Funding

This work was supported by the National Natural Science Foundation of China (grant number: 32201051, 32271339), and the Fundamental Research Funds for the Central Universities (grant number: 2412021QD015).

CRediT authorship contribution statement

Liangnan Cui: Conceptualization, Investigation, Methodology, Resources, Writing – original draft. **Jing Wu:** Investigation, Formal analysis. **Xiang Wang:** Investigation, Formal analysis. **Xiaotong Yang:** Software, Validation, Writing – review & editing. **Zixin Ye:** Software, Validation. **Kevin H. Mayo:** Writing – review & editing. **Lin Sun:** Supervision. **Yifa Zhou:** Resources, Supervision, Writing – review & editing.

Declaration of Competing Interest

The authors declare that they have no known competing financial interests or personal relationships that could have appeared to influence

the work reported in this paper.

Data availability

Data will be made available on request.

Appendix A. Supplementary data

Supplementary data to this article can be found online at https://doi.org/10.1016/j.fochx.2023.100706.

References

Bai, R., Zhang, Y., Jia, X., Fan, J., Hou, X., Wang, Y., … Hu, F. (2020). Isolation, characterization and immunomodulatory activity of oligosaccharides from Codonopsis pilosula. *Journal of Functional Foods, 72*, Article 104070. https://doi.org/10.1016/j.jff.2020.104070

Benhura, M. A. N., Mbuya, N., & Machirori, E. (1999). Facile formation of caramel colours using the polysaccharide material that is extracted from the fruit of Azanza garckeana. *Food Chemistry, 65*(3), 303–307. https://doi.org/10.1016/S0308-8146(98)00199-X

Catenza, K. F., & Donkor, K. K. (2021). Recent approaches for the quantitative analysis of functional oligosaccharides used in the food industry: A review. *Food Chemistry, 355*, Article 129416. https://doi.org/10.1016/j.foodchem.2021.129416

Chi, L., Khan, I., Lin, Z., Zhang, J., Lee, M. Y. S., Leong, W., … Zheng, Y. (2020). Fructo-oligosaccharides from Morinda officinalis remodeled gut microbiota and alleviated depression features in a stress rat model. *Phytomedicine, 67*, Article 153157. https://doi.org/10.1016/j.phymed.2019.153157

de Oliveira, A. J. B., Gonçalves, R. A. C., Chierrito, T. P. C., dos Santos, M. M., de Souza, L. M., Gorin, P. A. J., … Iacomini, M. (2011). Structure and degree of polymerisation of fructooligosaccharides present in roots and leaves of Stevia rebaudiana (Bert.) Bertoni. *Food Chemistry, 129*(2), 305–311. https://doi.org/10.1016/j.foodchem.2011.04.057

Dong, C., Zhang, L., Xu, R., Zhang, G., Zhou, Y., Han, X., … Sun, Y. (2015). Structural characterization and immunostimulating activity of a levan-type fructan from Curcuma kwangsiensis. *International Journal of Biological Macromolecules, 77*, 99–104. https://doi.org/10.1016/j.ijbiomac.2015.03.009

DuBois, M., Gilles, K. A., Hamilton, J. K., Rebers, P. A., & Smith, F. (1956). Colorimetric method for determination of sugars and related substances. *Analytical Chemistry, 28*(3), 350–356. https://doi.org/10.1021/ac60111a017

Fujishima, M., Furuyama, K., Ishihiro, Y., Onodera, S., Fukushi, E., Benkeblia, N., & Shiomi, N. (2009). Isolation and structural analysis in vivo of newly synthesized fructooligosaccharides in onion bulbs tissues (Allium cepa L.) during storage. *International Journal of Carbohydrate Chemistry*, *2009*, 493737. 10.1155/2009/493737.

Guo, Y., Yin, T., Wang, X., Zhang, F., Pan, G., Lv, H., … Wu, H. (2017). Traditional uses, phytochemistry, pharmacology and toxicology of the genus Cimicifuga: A review. *Journal of Ethnopharmacology, 209*, 264–282. https://doi.org/10.1016/j.jep.2017.07.040

He, L., Yan, B., Yao, C., Chen, X., Li, L., Wu, Y., … Luo, P. (2021). Oligosaccharides from Polygonatum Cyrtonema Hua: structural characterization and treatment of LPS-induced peritonitis in mice. *Carbohydrate Polymers, 255*, Article 117392. https://doi.org/10.1016/j.carbpol.2020.117392

Honda, C., Katsuta, R., Yamada, M., Kojima, Y., Mamiya, A., Okada, N., … Tokuoka, M. (2021). Novel glucoamylase-resistant gluco-oligosaccharides with adjacent α-1, 6 branches at the non-reducing end discovered in Japanese rice wine, sake. *Carbohydrate Polymers, 251*, Article 116993. https://doi.org/10.1016/j.carbpol.2020.116993

Hu, L., Song, X., Nagai, T., Yamamoto, M., Dai, Y., He, L., … Yao, Z. (2021). Chemical profile of Cimicifuga heracleifolia Kom. And immunomodulatory effect of its representative bioavailable component, cimigenoside on Poly(I:C)-induced airway inflammation. *Journal of Ethnopharmacology, 267*, Article 113615. https://doi.org/10.1016/j.jep.2020.113615

Ishiguro, Y., Ueno, K., Onodera, S., Benkeblia, N., & Shiomi, N. (2011). Effect of temperatures on inulobiose and inulooligosaccharides in burdock roots during storage. *Journal of Food Composition and Analysis, 24*(3), 398–401. https://doi.org/10.1016/j.jfca.2010.08.008

Mohapatra, S., Iqubal, A., Ansari, M. J., Jan, B., Zahiruddin, S., Mirza, M. A., … Iqbal, Z. (2022). Benefits of black cohosh (Cimicifuga racemosa) for women health: an up-close and in-depth review. *Pharmaceuticals, 15*, 278. https://doi.org/10.3390/ph15030278

Liang, L., Liu, G., Yu, G., Song, Y., & Li, Q. (2019). Simultaneous decoloration and purification of crude oligosaccharides from pumpkin (Cucurbita moschata Duch) by macroporous adsorbent resin. *Food Chemistry, 277*, 744–752. https://doi.org/10.1016/j.foodchem.2018.10.138

Liu, H., Wei, X., Zu, S., Lin, X., Zhang, J., Shi, A., … He, N. (2021). Separation and identification of neutral oligosaccharides with prebiotic activities from apple pectin. *Food Hydrocolloids, 121*, Article 107062. https://doi.org/10.1016/j.foodhyd.2021.107062

Moreno, F. J., Corzo, N., Montilla, A., Villamiel, M., & Olano, A. (2017). Current state and latest advances in the concept, production and functionality of prebiotic oligosaccharides. *Current Opinion in Food Science, 13*, 50–55. https://doi.org/10.1016/j.cofs.2017.02.009

Needs, P. W., & Selvendran, R. R. (1993). Avoiding oxidative degradation during sodium hydroxide/methyl iodide-mediated carbohydrate methylation in dimethyl sulfoxide. *Carbohydrate Research, 245*(1), 1–10. https://doi.org/10.1016/0008-6215(93)80055-J

Pöhnl, T., Böttcher, C., Schulz, H., Stürtz, M., Widder, S., Carle, R., & Schweiggert, R. M. (2017). Comparison of high performance anion exchange chromatography with pulsed amperometric detection (HPAEC-PAD) and ultra-high performance liquid chromatography with evaporative light scattering (UHPLC-ELSD) for the analyses of fructooligosaccharides in onion (Allium cepa L.). *Journal of Food Composition and Analysis, 63*, 148–156. https://doi.org/10.1016/j.jfca.2017.08.001

Prieto-Santiago, V., Cavia, M.d. M., Barba, F. J., Alonso-Torre, S. R., & Carrillo, C. (2022). Multiple reaction monitoring for identification and quantification of oligosaccharides in legumes using a triple quadrupole mass spectrometer. *Food Chemistry, 368*, Article 130761. https://doi.org/10.1016/j.foodchem.2021.130761

Qin, R., Lv, C., Zhao, Y., Zhao, Y., Yu, Y., & Lu, J. (2017). Assessment of phenolics contents and antioxidant properties in Cimicifuga dahurica (Turcz.) Maxim during drying process. *Industrial Crops and Products, 107*, 288–296. https://doi.org/10.1016/j.indcrop.2017.06.004

Ronkart, S. N., Blecker, C. S., Fourmanoir, H., Fougnies, C., Deroanne, C., Van Herck, J.-C., & Paquot, M. (2007). Isolation and identification of inulooligosaccharides resulting from inulin hydrolysis. *Analytica Chimica Acta, 604*(1), 81–87. https://doi.org/10.1016/j.aca.2007.07.073

Sedmak, J. J., & Grossber, S. E. (1977). A rapid, sensitive, and versatile assay for protein using coomassie brilliant blue G250. *Analytical Biochemistry, 83*(2), 788. https://doi.org/10.1016/0003-2697(77)90088-4

Shahidullah, M., & Khorasani, S. S. M. A. (1972). The sensitivity and selectivity of the Seliwanoff test for fructose. *Analytica Chimica Acta, 61*(2), 317–319. https://doi.org/10.1016/S0003-2670(01)95066-4

Shi, H., Xu, J., Wang, W., Jia, M., Zhou, Y., & Sun, L. (2020). An efficient protocol for the preparation of linear arabino-oligosaccharides. *Carbohydrate Research, 496*, Article 108131. https://doi.org/10.1016/j.carres.2020.108131

Shiomi, N., & Onodera, S. (1990). The ^{13}C-NMR Spectra of Inulo-oligosaccharides. *Agricultural and Biological Chemistry, 54*(1), 215–216. https://doi.org/10.1080/00021369.1990.10869895

Sims, I. M., Carnachan, S. M., Bell, T. J., & Hinkley, S. F. R. (2018). Methylation analysis of polysaccharides: Technical advice. *Carbohydrate Polymers, 188*, 1–7. https://doi.org/10.1016/j.carbpol.2017.12.075

Singh, R. S., Singh, R. P., & Kennedy, J. F. (2016). Recent insights in enzymatic synthesis of fructooligosaccharides from inulin. *International Journal of Biological Macromolecules, 85*, 565–572. https://doi.org/10.1016/j.ijbiomac.2016.01.026

Van den Ende, W. (2013). Multifunctional fructans and raffinose family oligosaccharides. *Frontiers in Plant Science, 4*, 247. https://doi.org/10.3389/fpls.2013.00247

Wang, S., Pan, J., Zhang, Z., & Yan, X. (2020). Investigation of dietary fructooligosaccharides from different production methods: Interpreting the impact of compositions on probiotic metabolism and growth. *Journal of Functional Foods, 69*, Article 103955. https://doi.org/10.1016/j.jff.2020.103955

Yang, X., Zhao, Y., He, N., & Croft, K. D. (2010). Isolation, characterization, and immunological effects of α-galacto-oligosaccharides from a new source, the herb Lycopus lucidus Turcz. *Journal of Agricultural and Food Chemistry, 58*(14), 8253–8258. https://doi.org/10.1021/jf101217f

Yang, Z., Hu, J., & Zhao, M. (2011). Isolation and quantitative determination of inulin-type oligosaccharides in roots of Morinda officinalis. *Carbohydrate Polymers, 83*(4), 1997–2004. https://doi.org/10.1016/j.carbpol.2010.11.006

Yuan, P., Shao, T., Han, J., Liu, C., Wang, G., He, S., … Chen, K. (2021). Burdock fructooligosaccharide as an α-glucosidase inhibitor and its antidiabetic effect on high-fat diet and streptozotocin-induced diabetic mice. *Journal of Functional Foods, 86*, Article 104703. https://doi.org/10.1016/j.jff.2021.104703

Zeng, H., Su, S., Xiang, X., Sha, X., Zhu, Z., Wang, Y., … Duan, J. (2017). Comparative analysis of the major chemical constituents in salvia miltiorrhiza roots, stems, leaves and flowers during different growth periods by UPLC-TQ-MS/MS and HPLC-ELSD methods. *Molecules, 22*, 271. https://doi.org/10.3390/molecules22050771

Zhang, R., Zhou, J., Jia, Z., Zhang, Y., & Gu, G. (2004). Hypoglycemic effect of Rehmannia glutinosa oligosaccharide in hyperglycemic and alloxan-induced diabetic rats and its mechanism. *Journal of Ethnopharmacology, 90*(1), 39–43. https://doi.org/10.1016/j.jep.2003.09.018

Zhang, Y., Zhuang, D., Wang, H., Liu, C., Lv, G., & Meng, L. (2022). Preparation, characterization, and bioactivity evaluation of oligosaccharides from Atractylodes lancea (Thunb.) DC. *Carbohydrate Polymers, 277*, Article 118854. https://doi.org/10.1016/j.carbpol.2021.118854

Zheng, Y., Li, L., Feng, Z., Wang, H., Mayo, K. H., Zhou, Y., & Tai, G. (2018). Preparation of individual galactan oligomers, their prebiotic effects, and use in estimating galactan chain length in pectin-derived polysaccharides. *Carbohydrate Polymers, 199*, 526–533. https://doi.org/10.1016/j.carbpol.2018.07.048